*The 2017 World Congress on*
***Advances in Structural Engineering and Mechanics (ASEM17)***
*28 August - 1 September, 2017, Ilsan(Seoul), Korea*

# Numerical analysis for diffusion induced crack patterns

*Sayako Hirobe[1)] and Kenji Oguni[2)]

[1), 2)] *Department of System Design Engineering, Keio University, Kanagawa 223-8522, Japan*
[1)] s.hirobe@keio.jp

## ABSTRACT

The desiccation cracks are formed as a consequence of the drying shrinkage of the materials. These cracks have a net-like structure and tessellate dry-out surfaces of the materials into polygonal cells. The previous experimental researches pointed out that the systematic change of the cell size depending on the layer thickness and the hierarchical pattern formation process are observed in the desiccation crack phenomenon.In this research, we consider that the water diffusion in the materials and the corresponding inhomogeneous drying shrinkage of the materials play an important role in the pattern formation of the desiccation cracks. According to this consideration, we model the desiccation crack phenomenon as a coupling of diffusion, deformation, and fracture. Based on this coupled model, we perform the numerical analysis for the reproduction of the desiccation crack pattern and its formation process by using the Particle Discretization Scheme Finite Element Method (PDS-FEM). The results of the numerical analysis show the satisfactory agreement with the experimental observations. Furthermore, we extend this coupled model to the crack patterns induced by the thermal diffusion (e.g., the ordered hexagonal cells seen in the columnar joint). Through the numerical analysis, we show that the governing mechanism for the pattern formation of the diffusion induced cracks is the coupling of diffusion, deformation, and fracture.

## 1. INTRODUCTION

The deformation induced by the volume change of the materials due to the diffusion of the moisture could result in the excessive stress and cracking of the materials. These cracks often damage to the foundation of the structures or the clayey liners used for the treatment of the nuclear waste. The prediction of the possibilities for such damages is still difficult, because the mechanism for the diffusion-induced cracks is not fully resolved.
The diffusion-induced cracks often form particular patterns, for instance, the net-like

---

[1)] Graduate Student
[2)] Professor

patterns of the desiccation cracks on the dry-out soil fields and the columnar joint in the cooling lava. In the previous researches, intensive effort has been paid for the investigation on the basic features of these particular patterns with various materials and conditions (Groisman and Kaplan 1994, Nahlawi and Kodikara 2006, Peron et al. 2008). The results of these researches imply that the pattern of the diffusion induced cracks have the typical length scale corresponding to the experimental conditions.

In the case of the desiccation cracks, the net-like cracks divide the drying surface into polygonal cells in the hierarchical manner. These cells have the typical size (i.e., the typical length scale) and this size changes systematically depending on the layer thickness. To show the relationship between the typical cell size and the layer thickness, some models and simulation methods have been proposed (Musielak and Śliwa 2012, Peron et al. 2008, Rodríguez et al. 2007, Sima et al. 2014, Vogel et al. 2005). While these models can reproduce the crack patterns similar to the experimental observations, the variation of crack patterns depending on the experimental conditions and the three-dimensional crack behavior cannot be reproduced. This might be because that their numerical analysis methods are not suitable for the fracture analysis or their models assume the homogeneous water distribution. These modeling and simulating difficulties seem to disturb the understanding the fundamental mechanism of the desiccation crack phenomenon.

The problems for the cracking behavior of the materials under diffusion induced deformation result in the coupled problems of the multi physics: the moisture/thermal diffusion, deformation due to the inhomogeneous volume change corresponding to the moisture/thermal distribution, and fracture. In this paper, the coupled model of diffusion, deformation, and fracture for the desiccation cracks is presented in the context of the continuum mechanics. Based on this coupled model, we perform the numerical analysis using PDS-FEM (Particle Discretization Scheme Finite Element Method) developed by the authors (Oguni et al. 2009, Wijerathne et al. 2009).

Through the numerical analysis for the desiccation cracks, we observe the crack propagation process, the particular pattern formation of cracks, and the emergence of the typical length scale of the crack pattern.

## 2. DRYING EXPERIMENT

We perform the drying tests of calcium carbonate slurry to observe the crack patterns and to measure parameters for the numerical analysis. The calcium carbonate slurry was prepared at volumetric water content 72%. The slurry was poured into the rectangular acrylic container (100×100×50 mm). For the observation of the change in the crack pattern depending on the layer thickness, the thickness of the slurry was set to 5 mm, 10 mm, and 20 mm. The slurry was dried in the air (20 °C temperature and at 50 % relative humidity) until the specimen dried out completely. The time history of the volumetric water content was measured during desiccation.

Figure 1 shows that the crack patterns formed on the top surface of the specimens with different thickness. In this figure, the net-like cracks are formed and polygonal cells are observed in all specimens. The size of these polygonal cells is kept almost constant in each thickness and the average cell size on the final pattern increases with the increase of the specimen thickness.

Figure 2 shows the crack propagation process on the top surface of the specimen with 10mm thickness. At the initial stage of the crack pattern formation (corresponding to Fig. 2 (a)-(c)), long cracks grow from the edge of the specimen and form the lager cells. These long cracks are neither branched nor curved hard but they are mildly-curved. Then, small cracks appear and divide the existing cells (corresponding to Fig. 2 (d)-(e)). The observed cracks tend to intersect at a right angle. Thus, the final crack pattern is formed through the hierarchical cell tessellation process.

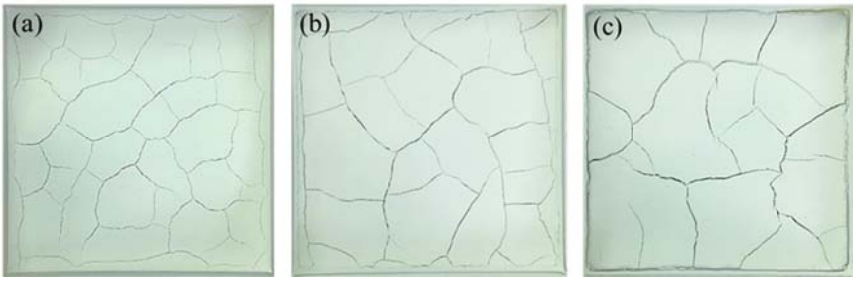


Fig. 1 The final crack patterns formed on the top surface of the specimens with different thickness. (a) 5mm, (b) 10mm, (c) 20mm

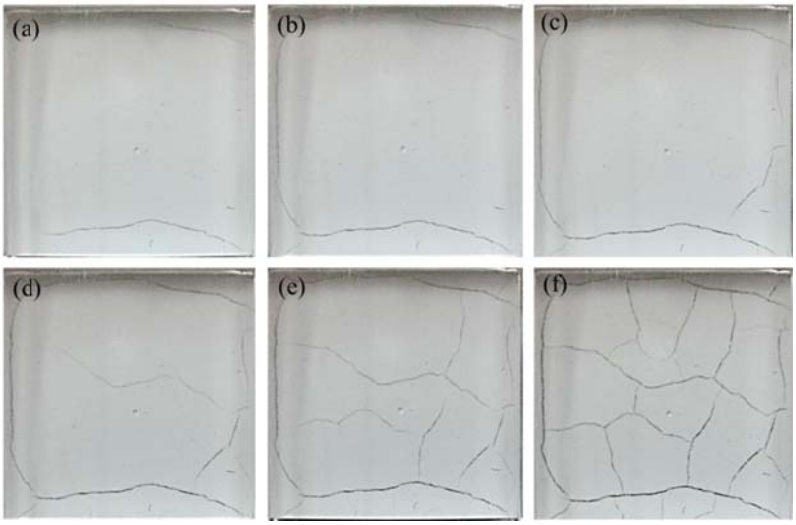


Fig. 2 Crack propagation process on the top surface of 10mm thickness specimen

## 3. MATHEMATICAL MODEL

The volume of the mixture of powder and the water changes depending on the water content. When the water evaporates from the top surface of the materials, the inhomogeneous water distribution and/or boundary constraints cause non-uniform drying shrinkage. This inhomogeneous volume change could generate the excessive stress resulting in the fracture. Thus, the desiccation crack phenomenon is regarded as the coupled problem of the moisture diffusion, deformation due to the inhomogeneous volume change corresponding to the moisture distribution, and fracture.

Assuming the mixture of the powder and the water as a permeable solid continuum, the water movement inside the mixture is given as the following initial boundary value problem:

$$\frac{\partial \theta}{\partial t} = D\nabla^2\theta \qquad \boldsymbol{x} \in \Omega \tag{1a}$$

$$D\frac{\partial \theta}{\partial \boldsymbol{n}} = -Q^1(\theta) \qquad \boldsymbol{x} \text{ on } \partial\Omega \tag{1b}$$

$$\theta(\boldsymbol{x},0) = \overline{\theta} \qquad \boldsymbol{x} \in \Omega \tag{1c}$$

where Eq. (1a) is Richards' equation under isothermal condition (Richards 1931), $\theta$ is a volumetric water content, $\Omega$ is a homogeneous linear elastic body, $D$ is a diffusion coefficient, $Q^1(\theta)$ is a water flux due to the evaporation from the external boundary $\partial\Omega$, and $\boldsymbol{n}$ is a unit normal vector to the external boundary $\partial\Omega$. Here, the volumetric water content $\theta$ is a function of position $\boldsymbol{x}$ and time $t$. Note that the diffusion coefficient $D$ is constant and the gravitational effect is ignored.

The effect of cracks on the water movement is introduced as (i) the evaporation from the crack surfaces, (ii) the shield for the water movement (the water cannot move across the crack surfaces). The first effect is introduced as the Neumann boundary condition for the initial boundary value problem (1):

$$D\frac{\partial}{\partial \boldsymbol{n}}\theta(\boldsymbol{x},t) = -Q^2(\theta) \qquad \boldsymbol{x} \text{ on } \Gamma. \tag{2}$$

Here, $\Gamma$ is the crack surfaces and $Q^2(\theta)$ is a water flux due to the evaporation from the crack surfaces. The second effect is introduced as follows: We set the water flux $\boldsymbol{J}_c$ as the projection of the water flux $\boldsymbol{J}$ on the crack surfaces. Only the tangential components of $\boldsymbol{J}$ on the crack surfaces survive after this projection. In the prime coordinate system $\{\boldsymbol{e}_i'\}$, $\boldsymbol{e}_3'$ is the unit normal vector of the crack surfaces. Then, $\boldsymbol{J}_c$ is written as Eq. (3) with the coordinate transform matrix $\boldsymbol{P}$ (defined as Eq. (4)) and the projection matrix $\boldsymbol{T}$ (defined as Eq. (4)):

$$J_i^c = T_{ji}P_{jk}T_{kl}J_l \tag{3}$$

$$T_{ij} = \boldsymbol{e}_i' \cdot \boldsymbol{e}_j \tag{4}$$

$$P_{ij} = \begin{cases} 1 & \text{if } i = j = 1, 2 \\ 0 & \text{otherwize.} \end{cases} \tag{5}$$

This removal of the water flux normal to the crack surfaces corresponds to the introduction of the anisotropic diffusion coefficient to the initial boundary value problem (1).

In the case of drying shrinkage, since the shrinkage strain $\varepsilon_{ij}^{s}$ is a result of the volume reduction, it does not generate stress. Instead, the elastic strain $\varepsilon_{ij}^{e}$, which is calculated by subtracting the shrinkage strain $\varepsilon_{ij}^{s}$ from the total strain $\varepsilon_{ij}$, generates the stress:

$$\varepsilon_{ij}^{e} = \varepsilon_{ij} - \varepsilon_{ij}^{s}. \tag{6}$$

The relationship between the change in the volumetric water content and the volumetric drying shrinkage strain $\varepsilon^{v}$ is

$$\varepsilon^{v}(\boldsymbol{x},t) = \frac{1}{\alpha}\frac{\rho_w}{\rho_d}\{\theta(\boldsymbol{x},0) - \theta(\boldsymbol{x},t)\} \tag{7}$$

where $\alpha$ is a moisture shrinkage coefficient of the powder, $\rho_w$ is the mass density of the water, and $\rho_d$ is a dry bulk density of the powder. Considering the homogeneity and isotropy of Ω, the drying shrinkage strain $\varepsilon_{ij}^{s}$ is

$$\varepsilon_{ij}^{s} = \frac{1}{3}\varepsilon^{v}\delta_{ij} \tag{8}$$

where $\delta_{ij}$ is a Kronecker's delta. According to Eq. (6), the strain energy for the drying shrinkage is defined as

$$I = \int_{\Omega}\frac{1}{2}\left(\varepsilon_{ij} - \varepsilon_{ij}^{s}\right)c_{ijkl}\left(\varepsilon_{kl} - \varepsilon_{kl}^{s}\right)dV \tag{9}$$

where $c_{ijkl}$ is an elastic tensor.

In this paper, we use the PDS-FEM for the seamless analysis of the deformation and the fracture. PDS-FEM is a fracture analysis method which can easily treat the discontinuous field due to fracture without introducing additional nodes or re-meshing. This method is to solve the boundary value problem for a continuum model of a deformable body with particle discretization of a displacement field. PDS-FEM applies the particle discretization to the physical field by using Voronoi tessellations $\{\Phi^{\alpha}\}$ and the conjugate Delaunay tessellations $\{\Psi^{\beta}\}$. The Delaunay tessellations are identical to the linear triangular or the tetrahedral elements used in ordinary FEM. The detailed explanation for PDS-FEM should be referred to Oguni et al. (2009) and Wijerathne et al. (2009). We apply this discretization scheme to the functional $I$ to evaluate numerically. To minimize discretized strain energy, displacement $u_i$ should satisfy the next equation of force equilibrium:

$$\sum_{\gamma=1}^{N} K_{ik}^{\alpha\gamma} u_k^{\gamma} = f_i^{\alpha} \tag{10}$$

$$K_{ik}^{\alpha\gamma} = \sum_{\beta=1}^{M} B_j^{\beta\alpha} c_{ijkl}^{\beta} B_l^{\beta\gamma} \Psi^{\beta} \tag{11}$$

$$f_k^{\alpha} = \varepsilon_{ij}^{s\beta}\left(c_{ijkl}^{\beta}\ B_l^{\beta\alpha}\right)\Psi^{\beta} \tag{12}$$

where $M$ is a number of Delaunay tessellations, $N$ is a number of Voronoi tessellations, $\Psi^{\beta}$ is the volume of $\beta$-th Delaunay tessellations, $B_i^{\beta\alpha}$ is a six-by-twelve strain-displacement matrix, and $K_{ij}^{\beta\gamma}$ is a stiffness matrix. The stiffness matrix $K_{ij}^{\beta\gamma}$ is equal to that of the ordinary FEM in spite of the different discretization. On Eq. (12), since $c_{ijkl}^{\beta}$ is a material constant, the external force vector $f_i^{\alpha}$ is uniquely-defined for each shrinkage strain $\varepsilon_{ij}^{s\beta}$. The external force vector $f_i^{\alpha}$ has a product of drying shrinkage strain $\varepsilon_{ij}^{s\beta}$ and space derivative operator $B_i^{\beta\alpha}$. This product implies that the source of external force (i.e., excessive stress) is a spatial derivative of shrinkage (i.e., inhomogeneous volume change).

## 4. NUMERICAL ANALYSIS

We perform the numerical analysis to reproduce the crack patterns and their formation process observed in the drying experiment of calcium carbonate slurry. We prepared three analysis models with different thickness as the drying experiment. The width and height of the model is set as 100 mm and the thickness $T$ is set as 5 mm, 10 mm, and 20 mm. The parameters are shown in Table 1. We assume the brittle fracture and the material constants (i.e., $\rho_d$, $\alpha$, $D$, $v$, $E$, $t_c$) is determined from the drying experiments performed by Peron et al. (2008). The boundary conditions are set as follows: the nodal displacement of the bottom surface and the sides are constrained in the all directions and the water evaporates only from the top surface; see Fig. 3. The initial volumetric water content is 0.56 (when the saturation degree is almost 100% in the drying experiment of calcium carbonate slurry) and the desiccation proceeds until the averaged volumetric water content reached to the 0.204. We prepared the finite element model with the unstructured mesh for each analysis model; see Table 2.

Based on the proposed coupled model, we perform the weak coupling analysis of FEM and PDS-FEM. The diffusion equation for the desiccation process is solved by ordinary FEM (with backward Euler method) and the equation of the force equilibrium for the deformation and fracture processes is solved by PDS-FEM with the constant time step 0.1 hour. When the maximum traction among the all elements reaches to the tensile strength $t_c$, the time step is reduced to 0.01 hour to capture the crack behavior promptly

**Table 1.** The parameters for the numerical analysis

| | |
|---|---|
| Soil dry density $\rho_d$ | 800 kg/m$^2$ hour |
| Evaporation speed on $\partial\Omega$ | $8.8\times10^{-5}$ m/hour |
| Evaporation speed on $\Gamma$ | $1.0\times10^{-5}$ m/hour |
| Initial volumetric water content | 0.560 |
| Moisture shrinkage coefficient $\alpha$ | 0.69 |
| Moisture diffusion coefficient $D$ | $3.6\times10^{-6}$ m$^2$/hour |
| Poisson's ratio $v$ | 0.3 |
| Young's modulus $E$ | 5.0 MPa |
| Tensile strength $t_c$ | 1.6 MPa |

**Table 2.** Mesh sizes for each analysis model

| Thickness *T* | Number of nodes | Number of elements |
|---|---|---|
| 5 mm | 253,930 | 50,355 |
| 10 mm | 278,337 | 51,726 |
| 20 mm | 309,509 | 61,146 |

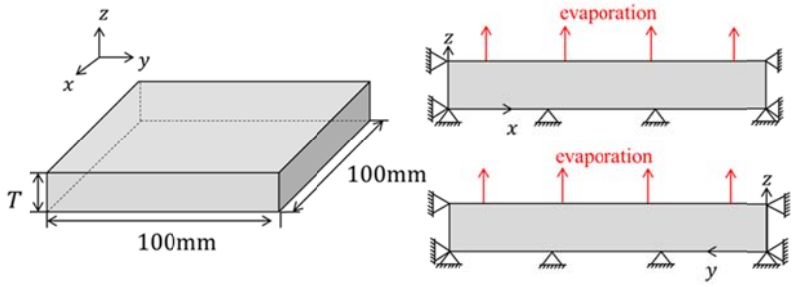


Fig. 3 The model and the boundary conditions for the numerical analysis.

The results of the numerical analysis are shown in Fig. 4 and Fig. 5. Figure 4 shows the final crack patterns formed on the top surface of the analysis model in each thickness. As seen in the result of the drying experiment of calcium carbonate slurry (Fig. 1), the net-like cracks appear and these cracks form the polygonal cells. The size of these cells is almost constant in each thickness. This cell size depending on the layer thickness is kept regardless of the choice of the initial mesh. Comparing the average cell size with different thickness, the average cell size increases as the increase of the model thickness. This qualitative tendency of the average cell size coincides with the experimental observation.

Figure 5 shows the crack propagation process on the top surface of 10mm thickness model. At the initial stage of the crack pattern formation, the long cracks extend and divide the top surface into larger cells (corresponding to Fig. 5 (a)-(c)). Then, short cracks appear between the existing cracks (corresponding to Fig. 5 (d)-(e)). This hierarchical cell tessellation process is also observed in the drying experiment of calcium carbonate slurry.

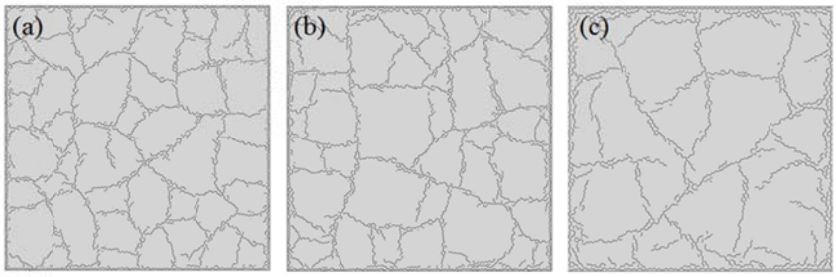


Fig. 4 The final crack patterns formed on the top surface of the analysis models with different thickness. (a) 5mm, (b) 10mm, (c) 20mm

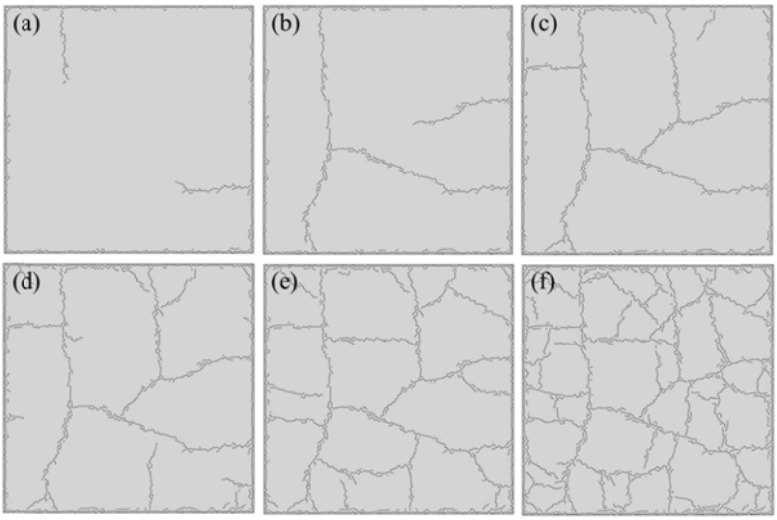


Fig. 5 Crack propagation process on the top surface of 10mm thickness model

## 5. CONCLUSION

In this paper, the coupling model of desiccation, deformation, and fracture for the desiccation crack phenomenon is proposed. By using this coupled model and appropriate numerical analysis method (weak coupling of FEM and PDS-FEM), we perform the numerical analysis to reproduce the crack patterns and their formation process observed in the drying experiment of calcium carbonate slurry.

The simulation results are qualitatively compared with the results of the drying test of calcium carbonate slurry. The simulation results show the satisfactory agreement with the experimental observation in terms of the net-like crack patterns, the formation process of the crack patterns, and the change in average cell size observed in the final pattern depending on the thickness of the desiccation layer. This agreement between the simulation results and the experimental observations indicates that the proposed coupling model of desiccation, deformation, and fracture can capture the fundamental mechanism for the desiccation crack phenomenon. To get more information about the pattern formation, we should relate the change of cell size to the parameters (e.g., depth, diffusion coefficient, tensile strength) quantitatively.

## REFERENCES

Groisman A. and Kaplan E. (1994), “An experimental study of cracking induced by desiccation,” *Europhys. Lett.*, **25**, 415-420.

Musielak G. and Śliwa T. (2012), “Fracturing of clay during drying: modelling and numerical simulation,” *Trans. Porous Med.* **95**, 465-481.

Nahlawi H. and Kodikara J.K. (2006), “Laboratory experiments on desiccation cracking of thin soil layers,” *Geotech. Geo.l Eng.* **24**, 1641-1664.

Oguni K., Wijerathne M.L.L., Okinaka T. and Hori M. (2009), "Crack propagation analysis using PDS-FEM and comparison with fracture experiment," *Mech. Mater*. **41**, 1242-1252.

Peron H., Delenne J.Y., Laloui L. and El Youssoufi M.S. (2008), "Discrete element modelling of drying shrinkage and cracking of soils," *Comput. Geotech.*, **36**, 61-69.

Peron H., Hueckel T., Laloui L. and Hu L.B. (2009), "Fundamentals of desiccation cracking of fine-grained soils: experimental characterization and mechanisms identification," *Can. Geotech. J.*, **46**, 1177-1201.

Richards LA (1931), "Capillary conduction of liquids through porous mediums," *J. Appl. Phys.*, **1**, 318-333

Rodríguez R., Sánchez M., Ledesman A. and Lloret A. (2007) "Experimental and numerical analysis of desiccation of mining waste," *Can. Geotech. J.*, **44**, 644-658.

Sima J., Jiang M., and Zhou C. (2014), "Numerical simulation of desiccation cracking in thin clayey layer using 3D discrete element modelling," *Comput. Geotech.*, **56**, 168-180.

Vogel H.J., Hoffmann H., Leopold A. and Roth K. (2005), "Studies of crack dynamics in clay soil II. a physically based model for crack formation," *Geoderma,* **125**, 213-223.

Wijerathne M.L.L., Oguni K. and Hori M. (2009), "Numerical analysis of growing crack problems using particle discretization scheme," *Int. J. Numer. Methods. Eng*., **80** 46-73.